

Probable detection of HI at $z \simeq 1.3$ from DEEP2 galaxies using the GMRT

Shiv K. Sethi¹, K. S. Dwarkanath¹, Chandrashekar Murugesan¹

Received _____; accepted _____

arXiv:1305.4017v1 [astro-ph.CO] 17 May 2013

¹Raman Research Institute, Bangalore 560080, India

ABSTRACT

We have observed the DEEP2 galaxies using the Giant Meterwave Radio Telescope in the frequency band of 610 MHz. There are $\simeq 400$ galaxies in the redshift range $1.24 < z < 1.36$ and within the field of view $\simeq 44'$, of the GMRT dishes. We have coadded the HI 21 cm-line emissions at the locations of these DEEP2 galaxies. We apply stacking on three different data cubes: primary beam uncorrected, primary beam corrected (uniform weighing) and primary beam corrected (optimal weighing). We obtain a peak signal strength in the range $8\text{--}25 \mu\text{Jy}/\text{beam}$ for a velocity width in the range $270\text{--}810 \text{ km sec}^{-1}$. The error on the signal, computed by bootstrapping, lies in the range $2.5\text{--}6 \mu\text{Jy}/\text{beam}$, implying a $2.5\text{--}4.7\text{-}\sigma$ detection of the signal at $z \simeq 1.3$. We compare our results with N-body simulations of the signal at $z \simeq 1$ and find reasonable agreement. We also discuss the impact of residual continuum and systematics.

Subject headings: galaxies: high-redshift—radio lines: galaxies—cosmology: observations

1. Introduction

To determine the evolution of the HI content of galaxies as a function of redshift is a very important input into the understanding of the history of gas content and star formation in the universe. While the study of damped Lyman-alpha clouds in absorption gives the evolution of the aggregate HI content in the redshift range $0.5 \leq z \leq 5$ (Prochaska et al. 2005; Rao et al. 2006; Noterdaeme et al. 2009, 2012), the determination of HI content of a halo of a given mass remains elusive at high redshifts owing to the faintness of individual halos in the HI 21 cm line emission, e.g. the detection of $\simeq 10^{10} M_{\odot}$ of HI at $z = 1.3$ would take 400 hours of observation with the Giant Meterwave Radio Telescope (GMRT) (Bagla et al. 2010). Direct observation of HI 21-cm line emission and its detailed modelling has only been possible at $z \simeq 0$ (Zwaan et al. 2005). For selected fields, the HI has been detected in emission for $z \lesssim 0.2$ (Verheijen et al. 2007; Verheijen et al. 2010; Catinella et al. 2008).

One possible approach to detect HI in emission at high redshifts rests on the detection of the fluctuation in the redshifted HI emission from high redshifts (Bharadwaj & Sethi 2001; Chang et al. 2008, Bharadwaj et al. 2009). Recently the first detection of HI at $z \simeq 0.7$ was reported based on cross-correlating the density field of optically-selected galaxies with known redshifts from the DEEP2 survey with the redshifted HI emission (Chang et al. 2010). This cross-correlation is non-zero only if HI is associated with galaxies observed by the DEEP2 survey; or this method detects the component of HI correlated with the DEEP2 galaxies. More recently, a detection at $z \simeq 0.8$ was reported based on the cross-correlation with WiggleZ galaxies (Masui et al. 2012). Stacking HI spectra of galaxies at known redshifts, akin to this approach, has also been attempted for both field and cluster galaxies at low redshifts (Lah et al. 2009; Lah et al. 2007).

Detailed N-body simulations (Khandai et al. 2011) showed that results of Chang et al (2010) can be consistently reproduced within the framework of density evolution in the

standard Λ CDM model. These simulations could estimate the possible range of bias and stochasticity of the HI density field, which are degenerate with the total HI content in the observation of Chang et al. (2010), and therefore directly estimate the HI content of the universe at $z \simeq 1$. These simulations also showed that stacking of HI 21 cm-line emission from galaxies of known redshifts can lead to a detailed reconstruction of the properties of HI halos at $z \simeq 1$. It was argued that GMRT could play an important role in this study both owing to its frequency coverage as well as its field of view.

In this letter we report GMRT observations of one of the DEEP2 fields and attempt to estimate the HI content of the universe at $z \simeq 1.3$ using stacking of the spectra at the locations of the DEEP2 galaxies.

Throughout this paper we use the spatially flat ($k=0$) Λ CDM model with $\Omega_m = 0.24$ and $h = 0.73$.

2. Observations and Data Analysis

DEEP2 redshift survey has made spectroscopic measurements of redshifts of over 25000 objects in the redshift range $0.7 < z < 1.5$, in four fields of approximate angular sizes $2^\circ \times 0.5^\circ$. Based on the examinations of the NVSS images of the the four DEEP2 Fields, the field centered at 1652+3455 (selected as 'Zone of very low extinction' for DEEP2 observations) was selected for observations with the GMRT at 610 MHz. Amongst the four fields, this field contains the minimum number of bright radio sources within the primary beams (full width at half maximum $\sim 44'$) of the GMRT antennas at 610 MHz. This will ensure that the images are least affected by dynamic range limitations of GMRT. In any case, dynamic range limitations will be minimal since this is a spectral line observation. This field, which is $2^\circ \times 0.5^\circ$ needs two GMRT pointings at 610 MHz. The desired velocity resolution is $\simeq 30 \text{ km s}^{-1}$ to detect signals with an expected width $\simeq 200 \text{ km s}^{-1}$. This velocity width

takes into account both the error in the redshift estimates of the DEEP2 galaxies and the expected velocity widths of the HI 21 cm-line signals. The velocity width of $\sim 30 \text{ km s}^{-1}$ corresponds to a channel width of $\sim 60 \text{ KHz}$ at 610 MHz.

Based on the distribution of DEEP2 galaxies in Right Ascension and Declination and in the redshift space, and taking into account the optimum range of frequencies for observations in the 610 MHz band, a frequency range of 601 to 633 MHz was selected. This frequency range corresponds to DEEP2 sources in the redshift range $1.24 < z < 1.36$, distributed over the range of right ascensions $251^{\circ}.6 < \alpha < 253^{\circ}.2$, and declinations $+34^{\circ}.65 < \delta < +35^{\circ}.2$. This region of $79' \times 33'$ was covered in two GMRT pointings, the primary beams (FWHM) of the GMRT dishes being $\sim 44'$. Each of these pointings were observed for a total of 12 hr with a bandwidth of 32 MHz and 512 channels. This setting gives a velocity resolution of $\sim 31 \text{ km s}^{-1}$. One of the two 12 hour pointings was completely analysed and is discussed below.

Corrupted data due to non-working antennas and baselines and due to the radio frequency interference were flagged using different tasks in the Astronomical Image Processing Software (AIPS). The data quality was good with less than 10 % of the data being flagged. A multi-channel continuum data set (32 channels) was formed from the spectral line data (512 channels) by averaging over 16 channels. This continuum data set was used to produce the best continuum images of this field. The continuum images so obtained had an RMS value of $85 \mu\text{Jy}/\text{beam}$ for a circular synthesised beam of $10''$. This image is dynamic range limited at a value ~ 3200 , as is usually the case with most GMRT continuum images.

The gain (complex) solutions obtained above were transferred to the spectral line data set. The continuum in the spectral line data was subtracted in two steps. First, the continuum source components that made the best continuum images were subtracted from the spectral line data set (task UVSUB in AIPS). Second, a second-order base line across

frequencies was fit to the resulting spectral line data set and was subtracted from the spectral line data set (task UVLSF in AIPS). This procedure yielded a continuum-free data set which was analysed for spectral features. A spectral line image cube (512 channels) with a spatial resolution of $10''$ and a spectral resolution of 30.7 km s^{-1} was produced. This spectral line image cube has an RMS of $260 \mu\text{Jy}/\text{beam}/\text{channel}$, close to the expected value of $\sim 200 \mu\text{Jy}/\text{beam}/\text{channel}$.

3. Results

From the image cube, we extract spectra at the positions of DEEP2 sources in the field of view. We then shift and add the spectra centered at the respective redshifts of the DEEP2 sources. In this procedure, we retain 50 channels on either side of the center of addition. If a source lies within 50 channels from the edges of the cube, it is excluded from the analysis. This process retains 489 sources out of a total of 539 for the entire field of view. We also apply primary beam correction to the image cube. This process increases the noise and the source flux away from the phase center. For the primary beam corrected cube, we retain sources only within 30% of the primary beam. There are 389 sources in this angular area and the procedure of coadding yields 371 sources.

We present results from both the primary-beam uncorrected and the primary-beam corrected cubes. To take into account this variation in the noise properties we coadd signal with both uniform and optimal weighting. In optimal weighting, the spectra are coadded with weights inversely proportional to the square of the noise in each spectra. The uniform weighting gives us an unbiased estimate of the signal (average peak flux of the halos) and allow us to compare the flux with theoretical estimates. The optimal weighting maximizes the signal-to-noise of the detection but constitutes a biased estimate of the signal. The

estimated signal strength in the three cases can be written as:

$$\begin{aligned}
 S_{\text{uncorr}} &= \frac{\sum_i S_i}{N} \\
 S_{\text{corr}} &= \frac{\sum_i S_i/w_i}{N} \\
 S_{\text{opt}} &= \frac{\sum_i S_i/(w_i\sigma_i^2)}{\sum_i 1/\sigma_i^2}
 \end{aligned}
 \tag{1}$$

Here S_i is the signal at the position of DEEP2 galaxies; σ_i is the noise in the spectrum at the position of DEEP2 galaxies, and w_i corresponds to the primary beam correction at the location of the galaxy.

The primary beam uncorrected analysis allows us to study the noise characteristics of the cube, while the corrected cases gives us a realistic estimate of the strength of the spectral line.

In Figure 1, we show the coadded raw spectrum and the 7-channel running average spectrum, from the primary beam uncorrected and the primary beam corrected image cubes.

3.1. The signal strength

In this paper we aim to measure the line flux and its velocity width of the stacked HI signal. In a detailed N-body simulation, Khandai et al. (2011) constructed several models of HI distribution at $z \simeq 1$ and computed the stacked spectra. All these models were normalized to the cumulative HI content Ω_{HI} as estimated by absorption studies, but were based on a range of HI mass functions, and therefore differed in emission properties of the signal. The stacked spectra obtained from these models show a peak flux between 10–30 μJy and velocity widths in the range 500-1000km sec $^{-1}$.

To extract the relevant information from the coadded signal, we average the signal with three velocity widths. Figure 2 shows the coadded spectra averaged over 9 points every

10th channel. Each of the nine points on the red (dashed) curve in the Figure corresponds to signal added for $(14 + 9i) \pm 4$ for i running from 0 and 8; the velocity width of the nine point averaging is 270 km sec^{-1} . Figure 3 and 4 show the signal averaged over 19 channels ($(12 + 19i) \pm 9$ for i from 0 to 4; velocity width 570 km sec^{-1}) and 29 channels ($(21 + 29i) \pm 14$, velocity width 770 km sec^{-1}), respectively. The choice of these three velocity averaging schemes allows us to estimate the velocity width of the central enhancement and also gauge the contribution of residual continuum and systematics on the wings of the line.

As noted above we present analysis of three different cubes of estimating the coadded signal (Eq 1). The interpretation of the signal in the three cases needs to be discussed. In the primary beam uncorrected case, the signal is dominated by halos close to the primary beam phase center. In the primary beam corrected uniform-weighting all the halos receive equal weight. In the optimal-weighting case, the signal is dominated by halos closer to the primary beam phase center as the halo flux is weighted as the square of the inverse of the noise which increases away from the phase center when the primary beam correction is made. This also means that one generically expects the signal in this case to be closer to the estimate of the primary beam uncorrected case, as we also find. It should be noted that the optimal case also give us an unbiased estimate of the signal if the HI signal from all the haloes is the same.

The signal strengths obtained for varying velocity widths using three different data cubes are given in Table 1.

3.2. Estimate of error on the signal

We adopt three different methods for estimating the error on the signal strength.

- (a) The most obvious method to make an estimate of the error on the signal is to estimate the RMS of the coadded signal (Figure 1) after appropriate velocity averaging

(Table 1). While this is the simplest approach to computing the error on the signal, it has severe limitations. For a nine-point average, we are left with only nine points to compute the signal and the noise; we do not quote this number for the other two velocity averaged spectra.

- (b) We scramble the redshifts of DEEP2 galaxies and adopt the same procedure for coadding the spectra as outlined above (9, 19, 29-point averaged, red, dashed curve in Figure 2, 3, and 4).

This procedure randomizes galaxy positions (in redshift space) and therefore should yield a null result; it can also act to suppress systematics in the original coadded spectra. We use this bootstrapping procedure to obtain 180–200 different realizations of the spectrum (20, 40, 60 realizations of 9-, 19- and 29- channel averaged spectra, each containing 9, 5, or 3 points), which enables us to obtain an estimate of the error in the signal. We check for convergence in each case.

For instance, in Figure 2, we show the average and RMS for 9 spectral point for 20 realizations obtained by scrambling DEEP2 galaxy redshifts. As all these spectral points are equivalent we could use all the 180 points to compute the error on the signal strength. Using all the 180 spectral points, we obtain an RMS of (4.3,10, 4.1) μJy from these spectra for the primary beam uncorrected and corrected (uniform and optimal) cubes, respectively (Table 1). Similar procedure is applicable for the other two velocity widths and the relevant results for these cases are shown in Figure 3 and 4 and Table 1.

The bootstrapping procedure described above acts to redistribute line flux across the entire data and while this suppresses the central enhancement it could also create a small line-flux bias which results in non-zero average for the coadded spectrum. The strength of this bias can be computed: as noted above we do not source lying within 50 channels on either side of spectrum, which leaves us with 412 spectral channels.

We randomize the redshift of the object for each spectra and follow the coadding process. The number of sources is $\simeq 400$ and the average line flux is $\simeq 20 \mu\text{Jy}$ with a velocity width corresponding to 20 channels (e.g. Figure 3). This flux is redistributed across $\simeq 412 \times 400$ channels, which results in the maximum line-flux bias of $\simeq 1 \mu\text{Jy}$ for the entire cube.

The probability of the scrambled signal to exceed the central enhancement is another indicator of the significance of the detection. However, when the number of realizations exceed the total number of data points the spectral channels get correlated and we do not get independent information of this significance. The total number of data points is the number of velocity-averaged spectral points for one spectrum multiplied by the the number of sources, which gives roughly 10000, 5000, and 3000 data points for the 9-, 19- and 29-channel averaging. When the number of realizations exceed these numbers we get spectral correlation, which prevents a statistical interpretation of our results. This also means that this procedure cannot give more than a 3.5σ detection (for a normal distribution).

This procedure gives us another measure of the significance of the signal. We run a large number of realizations (over 1000) to understand the nature of the signal in each case. Our findings are in broad agreement with the results shown in Table 1: (a) an increase in signal-to-noise for optimal weighting (we did not find a single instance in which the bootstrapped signal exceeded the central enhancement in such cases), (b) the signal-to-noise is maximum for 19-channel averaging case, (c) for cases where the signal-to-noise is expected to be smaller than 3σ , e.g. primary beam corrected, 29-channel averaged case, the results from this procedure are in agreement with Table 1.

- (c) The methods (a) and (b) do not take into account the noise properties of the whole data cube, which could be affected by other systematics. To determine the level of

homogeneity of noise along lines of sights that do not contain DEEP2 sources (Blank positions), we use the data along 40000 lines of sights towards these blank positions. These blank positions are randomly chosen and are separated from the positions of DEEP2 sources by more than a few synthesized beams. These spectra can be used to obtain many realizations of coadded spectra for the required number of sources. We apply exactly the same coaddition procedure on a set containing 500 such spectra as for the spectra containing the DEEP2 galaxies. We thus obtain 80 realizations of such coadded data sets towards blank positions, which are shown in Figure 5.

The average RMS of these raw spectra is $\simeq 12.6 \mu\text{Jy}$; the error on this RMS is $\simeq 0.8 \mu\text{Jy}$. The small error on the RMS shows that the noise properties of the data cube are stable and robust.

The average RMS for the 9, 19, and 29 channel averaged spectra is $\simeq \{4.4, 3, 2.3\} \mu\text{Jy}$, respectively (Table 1).

Information from blank positions can be used to estimate the level of significance of the detection in the direction of DEEP2 galaxies. We estimate the probability for the signal (for 9-, 19-, or 29-channel averaging) in the blank positions to exceed the central enhancement detected in the direction of DEEP2 galaxies. We find this probability to lie between 0.01–0.03 for the three cases of channel averaging. It is lowest for the 29-channel average and is comparable for the other two cases. The estimated probability correspond to between 2-2.5 σ detection of the signal for the primary beam uncorrected cube.

This procedure can not be used for the primary beam corrected cube as the noise increases away from the pointing center and therefore is not homogeneous across the cube.

3.3. Total line flux, residual continuum, and systematics

The results are displayed in Table 1 and Figure 2, 3, 4 can be briefly summarized as: (a) The signal strength is almost the same for both 9 and 19 channel averages but it falls for 29 channel average; 30% fall in the signal suggests the signal peaks within a velocity width of 570 km sec^{-1} (19-channel average), but there is detectable flux for velocity width $\simeq 1000 \text{ km sec}^{-1}$. (b) the maximum signal-to-noise is obtained for the velocity width $\simeq 570 \text{ km sec}^{-1}$, (c) residual flux is seen on the wings of the coadded spectra in almost all cases, in particular in the primary-beam corrected cases.

It is conceivable that the presence of residual flux is owing to the width of the signal being wider than 1000 km sec^{-1} , even though it is not supported by simulations (Khandai et al 2011). However, this hypothesis is less tenable because we do not see significant flux for the primary-beam uncorrected case, even though the central enhancement is prominent. A more likely hypothesis is that the residual flux in the line wings has other origins: (a) presence of unsubtracted continuum, (b) systematics in spectral domain picked while correcting for the primary beam and possible edge effects.

The impact of edge effects is seen in Figure 1 and also slightly discordant first and final channel fluxes for the three different velocity-averaged spectra (Figures 2–4). For 9-, 19-, and 29-channel averages we use channels: 10–90, 3–97, 7–93. We detect some edge effects which are seen in particular in the 19-channel averaging which uses information from channels closer to the edge.

We consider the 29-channel averaged spectrum to estimate the level of continuum residual and systematics in the coadded spectra. The average flux of all the channels except the central channel (average over 50 ± 14 channel) is: (0, 10, 6.7) μJy for the primary-beam uncorrected, corrected, and optimal case, respectively. The bootstrapping method redistributes the line flux and also serves to remove systematics but it leaves the

level of continuum unchanged. Therefore, the average of bootstrapped spectral points gives us an estimate of the level of residual continuum (Figure 3); this average is: (1.4, 4.4, 1.7) μJy for the primary-beam uncorrected, corrected, and optimal case, respectively.

It follows that the level of flux in the line wings is more than the residual continuum. As already noted above, the primary-beam uncorrected cube has relatively low levels of flux on the wings and the subtraction of residual continuum flux removes the flux on the wings below 1σ (Table 1). However, in the primary beam corrected uniform and optimal-weighting cases the average flux on the wings is still significant, which tends to suggest detectable flux even in the line wings at $1.5\text{--}2\sigma$ levels. For instance, we compute the probability of the flux level seen in the line wings in the highest signal-to-noise case: 19-channel averaged cube weighted optimally (Figure 3) by using bootstrapping method, we find the probability to be $\simeq 0.05$, roughly corresponding to a 2σ detection. However, the analysis of the primary beam uncorrected case clearly suggests that the line wing flux is attributable to a mix of residual continuum flux and systematics. The presence of systematics is also seen in the asymmetrical shape of the lines.

To get a conservative estimate of the signal, we assume that there is no flux in the cube for velocity widths exceeding the 29-channel average, and remove the flux in the line wings estimated from the 29-channel averaged spectra from all the channels in the corresponding cubes. The error on the central enhancement is obtained by the bootstrapping method (Table 1). Our final results are shown in Figure 6 for all the cases and they can be summarized as:

1. The signal-to-noise is maximum for the 19-channel averaging case and it lies in the range 2.7–4.7.
2. The signal-to-noise is the lowest for the 29-channel averaging case and is in the range 1.8–3.

3. As expected, the signal-to-noise is maximum for the optimally-weighted case.

4. Interpretation and Conclusions

We can directly compare our results with the simulations of Khandai et al. (2011). Their results showed that the stacked signal could have peak strength varying between 10–30 μJy and velocity width in the range 500–1000 km sec^{-1} (Figure 5 of their paper).

Khandai et al. (2011) considered many models, for the global HI content corresponding to $\Omega_{\text{HI}} = 10^{-3}$, to represent the HI content of the DEEP2 galaxies at $z \simeq 1$, based on different mass cuts on the dark matter haloes (e.g. Figure 7 of their paper). Our results are in agreement with their model 2 and 3, corresponding to a mass cut-off on the dark matter haloes in the range 10^{12} – $10^{12.5} M_{\odot}$. For these model, the line flux peaks in the range $\simeq 20$ – $30 \mu\text{Jy}$ and falls by roughly a factor of 10 within a velocity width of 800–1000 km sec^{-1} from the line center. This also means that the HI mass function at $z \simeq 1$ is more skewed towards the higher mass end as compared to the $z \simeq 0$ mass function (Zwaan et al. 2005); for detailed discussion, see Khandai et al. 2011).

Uncertainties in the estimate of HI content of the universe at $z \simeq 1$ partly arises from the fact that at this redshift the Lyman- α line is not directly accessible to ground based telescopes. At this redshift, the determination of the global HI content is enabled by HST observations, observation of associated MgII absorbers (Rao et al. 2006), the detection of HI in absorption against bright radio sources (Kanekar et al. 2009) and, more recently, through the cross-correlation of optical galaxies with redshifted HI emission (Chang et al. 2010). All these methods yield the HI content of the universe at $z \simeq 1$, $\Omega_{\text{HI}} \simeq 10^{-3}$ is roughly constant up to $z \simeq 4$ (Noterdaeme et al. 2012, Rao et al 2006).

Our result can potentially be interpreted in two possible ways: either the value of Ω_{HI} is higher than indicated by absorption studies or the DEEP2 galaxies provide a data set

biased towards higher HI masses. The simulations of Pontzen et al.(2008) suggest that damped Lyman- α systems are housed in dark matter halos of masses smaller than $10^{11} M_{\odot}$; from the measurement of mass-to-light ratio of DEEP2 galaxies, these galaxies are in dark matter halos almost an order of magnitude more massive, (Khandai et al. 2011, Figure 6). Alternatively, the mass function of the HI halos is tilted towards higher masses as compared to low redshifts. As noted above, a comparison of our results with the simulations of Khandai et al (2011), suggests that our results can be interpreted as arising from a HI mass distribution skewed towards the higher mass end, without invoking any enhancement in the global HI content. However, it is possible that the result could be partially owing to the uncertainty in the HI content at $z \simeq 1.3$.

In conclusion: we report the first tentative detection of HI at $z \simeq 1.3$. Our results are based on GMRT observation of DEEP2 fields and the coaddition of the signals at the locations of these galaxies. If confirmed, this would be the highest redshift at which the HI has been detected in emission. These results can be understood within the framework of existing data on the global HI content at $z \simeq 1$ and detailed modelling of HI at this redshift based on N-body simulations.

Currently, we are analysing GMRT data for additional DEEP2 fields and will obtain more data in the coming GMRT cycle. We aim to put our results on a firmer footing by a detection at a higher level of significance.

Table 1. HI Line results

	Uncorrected		Corrected		Corrected	
			(Uniform)		(optimal)	
	(μJy)		(μJy)		(μJy)	
9-channel average						
	Signal	Noise	Signal	Noise	Signal	Noise
DEEP2 galaxies	16.1	6.4	34.6	11.8	22.2	7.6
Random sight lines	NA	4.4	NA	NA	NA	NA
Scrambled redshifts	NA	4.3	NA	10	NA	4.1
19-channel average						
	Signal	Noise	Signal	Noise	Signal	Noise
DEEP2 galaxies	13.2	NA	32.9	NA	21.6	NA
Random sight lines	NA	3.4	NA	NA	NA	NA
Scrambled redshifts	NA	3.8	NA	8.6	NA	3.1
29-channel average						
	Signal	Noise	Signal	Noise	Signal	Noise
DEEP2 galaxies	9.2	NA	24	NA	15.7	NA
Random sight lines	NA	2.8	NA	NA	NA	NA
Scrambled redshifts	NA	3.4	NA	7.5	NA	2.8

Note. — The first three rows give the results based on 9 channel averaging. The

First column computes the average and the RMS from the coadded spectrum containing DEEP2 galaxies. The second row gives the noise estimates based on the 40000 random lines of sight. The third row gives the error when DEEP2 galaxy redshifts are scrambled. The other rows present results for the other two velocity-averaged spectra

Acknowledgement

We thank Rajaram Nityananda for many useful suggestions and the staff of the GMRT who have made these observations possible. The GMRT is run by the National Centre for Radio Astrophysics of the Tata Institute of Fundamental Research.

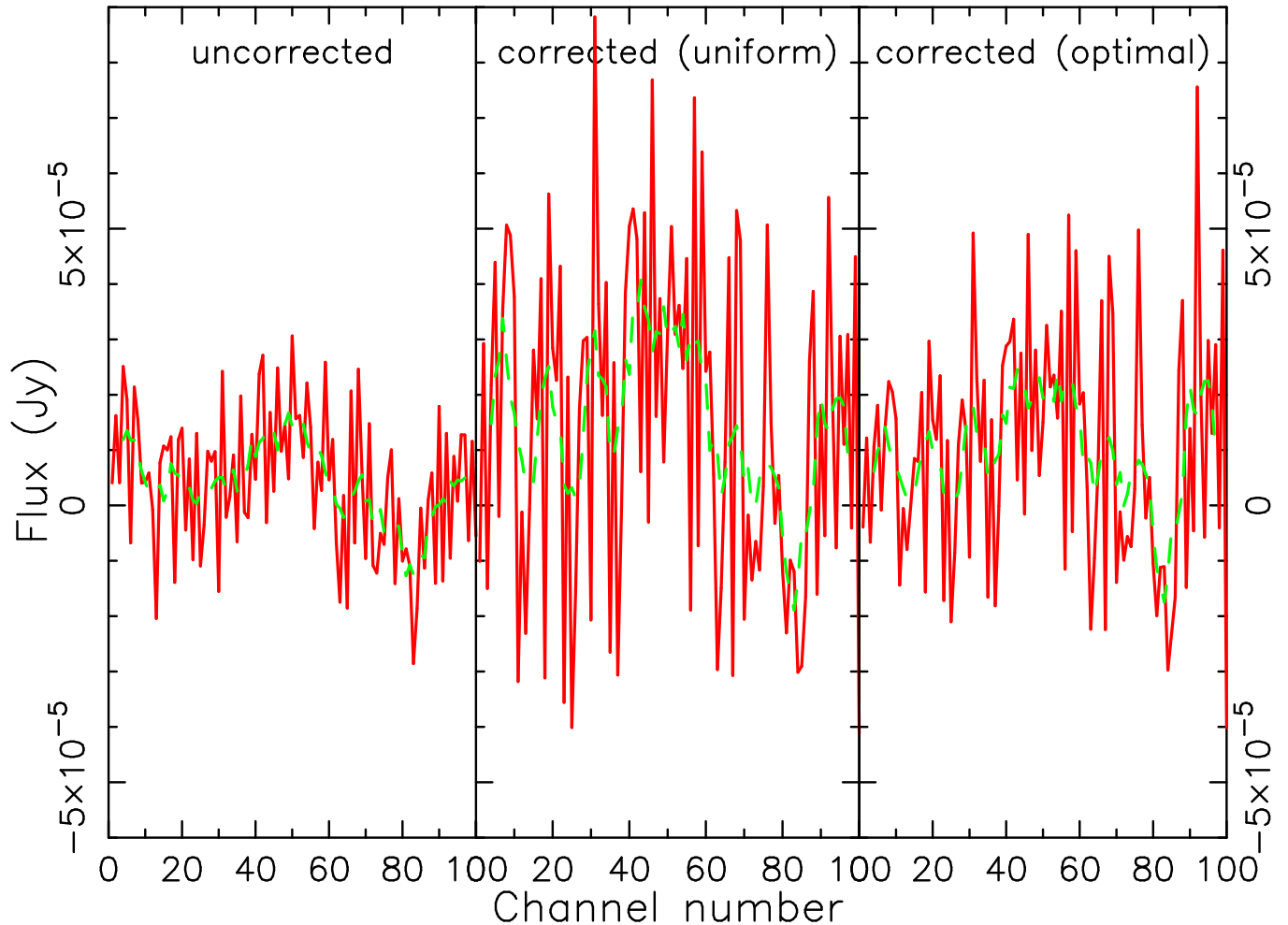


Fig. 1.— Co-added spectra toward DEEP2 galaxies. Left panel: The spectra are shifted and coadded at the central channel (number 50). The coadded spectrum contain 489 sources. The two curves correspond to: raw (solid, red), running average of 7 channels (dashed, green). The channel width is $\simeq 30 \text{ km s}^{-1}$. Middle and Right panels: The same as the Left panel for primary beam corrected cube for uniform and optimal weighing, respectively. There are 371 sources in the coadded spectrum.

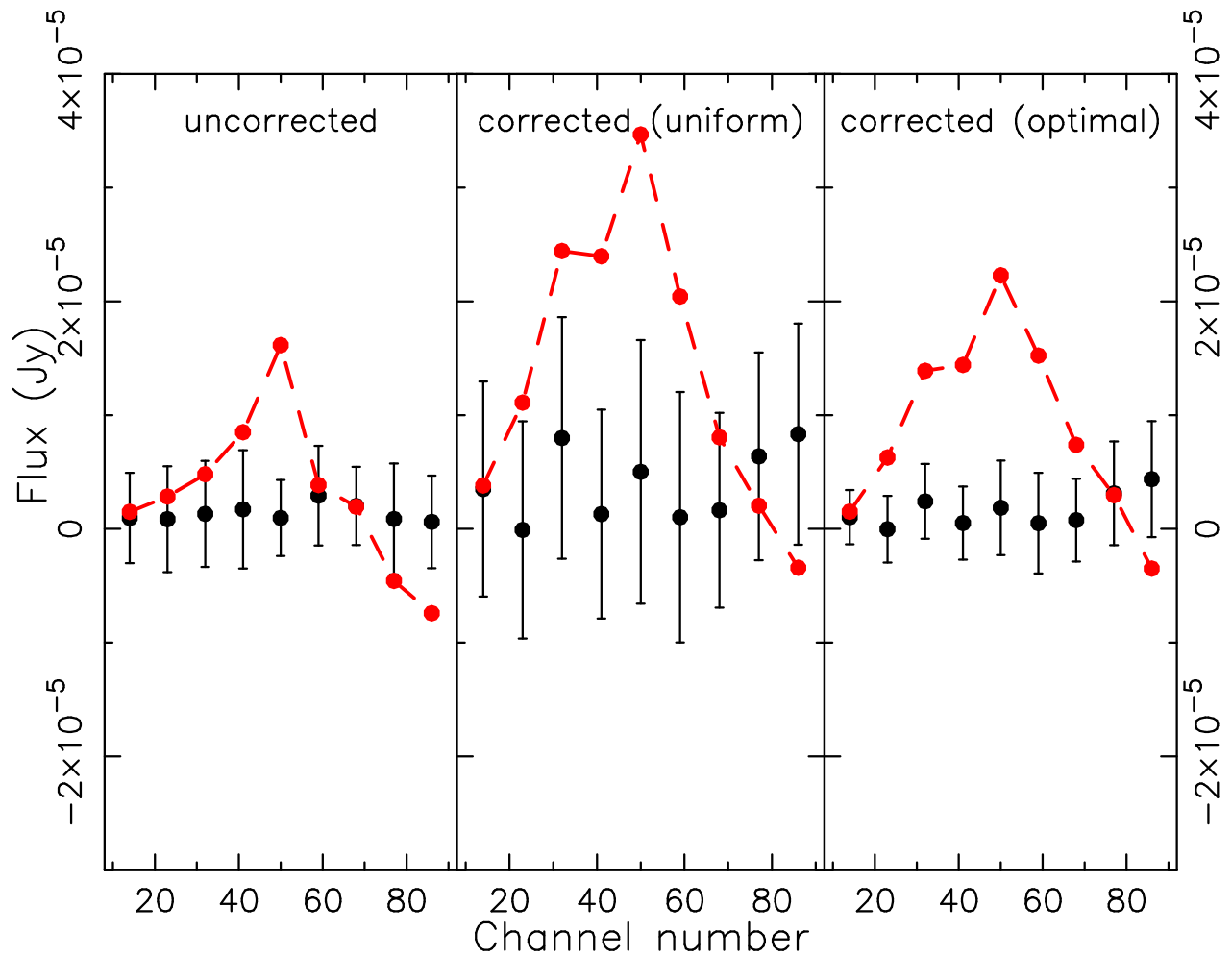


Fig. 2.— Co-added HI signal toward the DEEP2 galaxies. The red dashed line shows the signal obtained from coadding and averaging over 9 channels. The data points and errors shown are obtained by computing the mean and the RMS of 20 realizations at each spectral point, from realizations obtained by scrambling the redshifts of DEEP2 galaxies. The Left, center, and right panels correspond to primary beam uncorrected, corrected (uniform), and corrected (optimal) cases, respectively

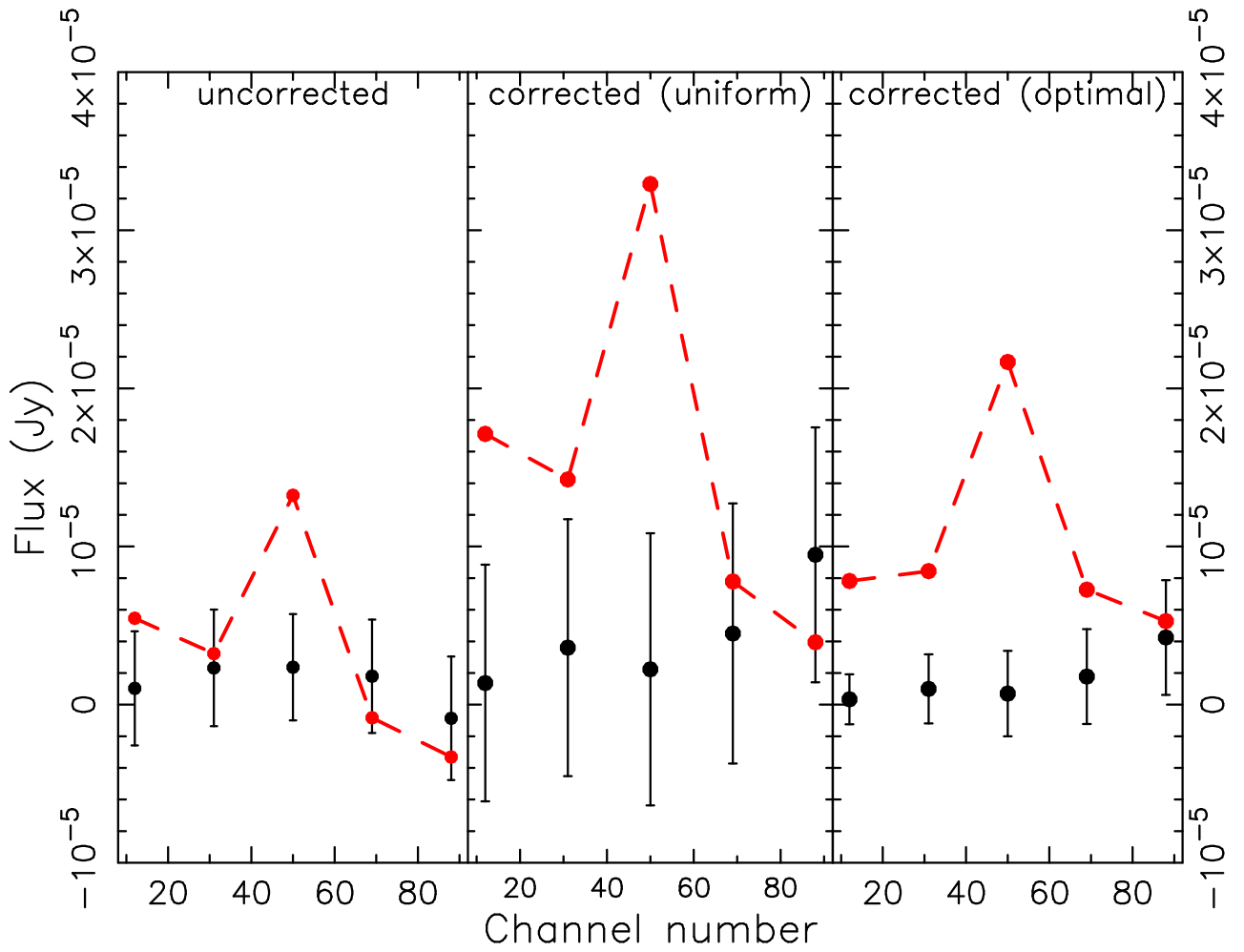


Fig. 3.— Co-added HI signal toward the DEEP2 galaxies. The red dashed line shows the signal obtained from coadding and averaging over 19 channels. The data points and errors shown are obtained by computing the mean and the RMS of 40 realizations at each spectral point, from realizations obtained by scrambling the redshifts of DEEP2 galaxies.

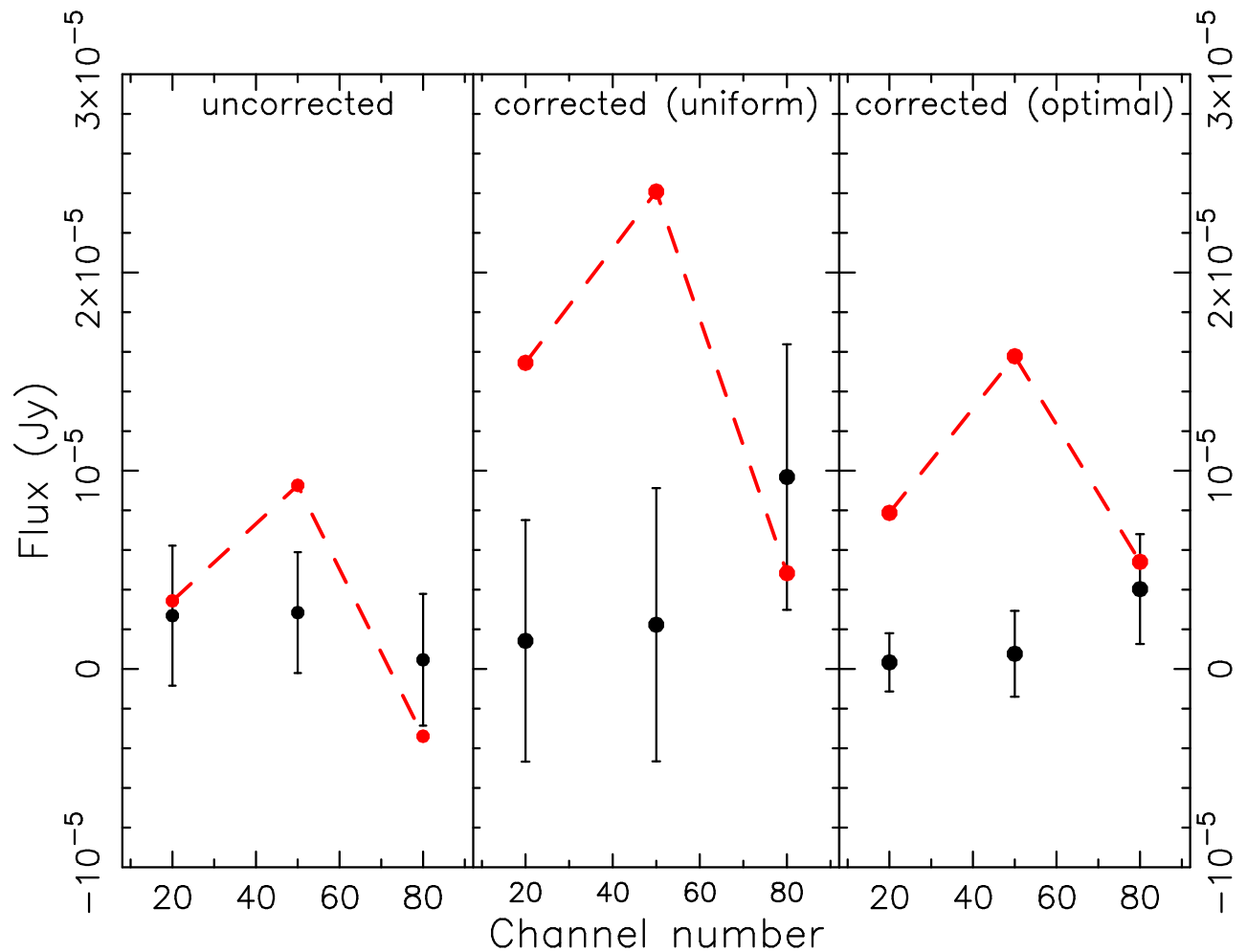


Fig. 4.— Co-added HI signal toward the DEEP2 galaxies. The red dashed line shows the signal obtained from coadding and averaging over 29 channels. The data points and errors shown are obtained by computing the mean and the RMS of 60 realizations at each spectral point, from realizations obtained by scrambling the redshifts of DEEP2 galaxies.

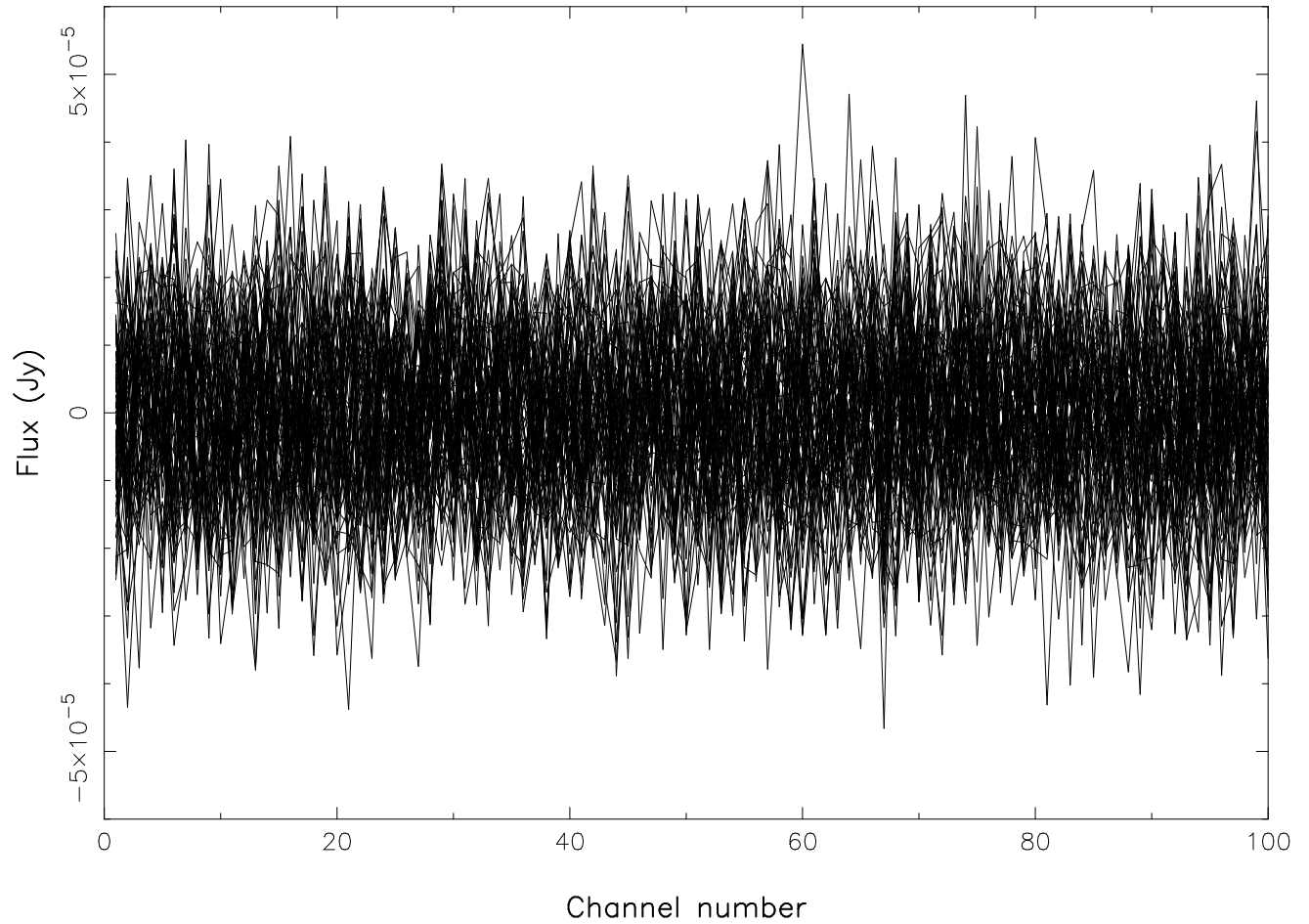


Fig. 5.— Noise in the cube toward blank positions. Coadded spectra for 80 realizations (total 40000 sources, each realization contains the coadded spectra of 500 sources) obtained from random lines of sights from the primary beam uncorrected cube.

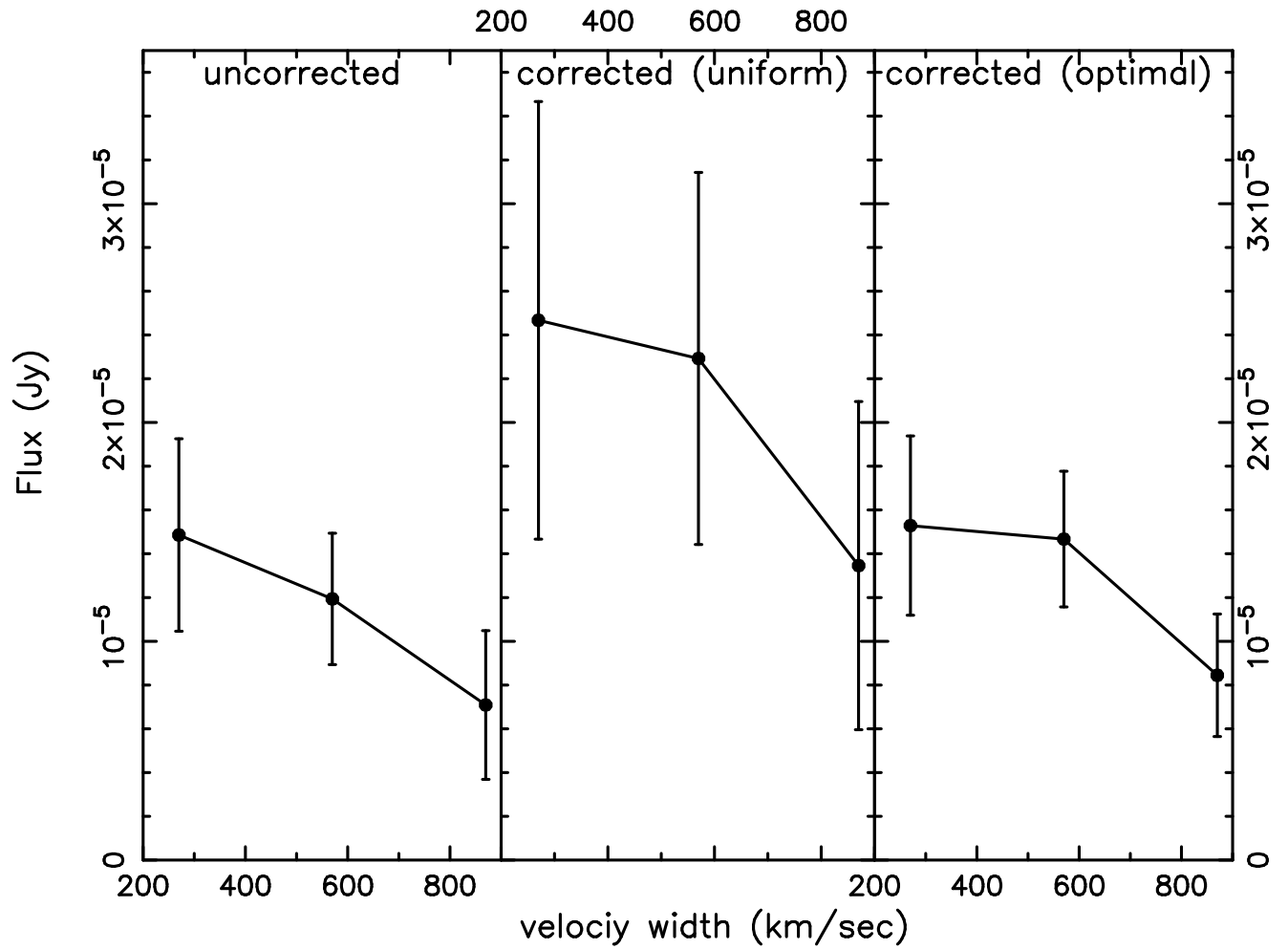


Fig. 6.— The change in peak flux as a function of velocity width is shown for the three data cubes.